

HD-A133 119

PROGRAM IN MARINE PHYSICS APPLIED TO NAVY UNDERSEA
MISSIONS (U) SCRIPPS INSTITUTION OF OCEANOGRAPHY LA
JOLLA CA MARINE PHYSIC. V C ANDERSON ET AL.

1/1

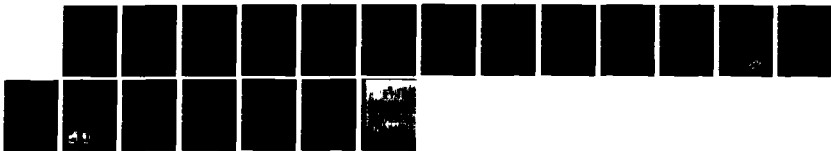
08 JUN 83

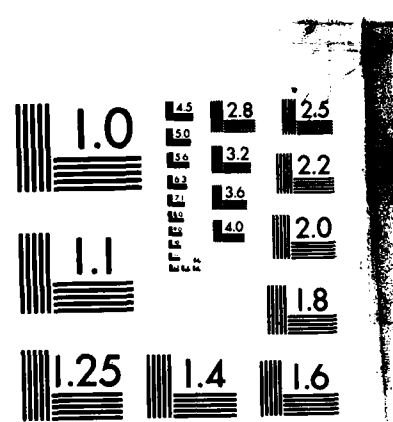
UNCLASSIFIED

MPL-U-42/83 N00014-80-C-0077

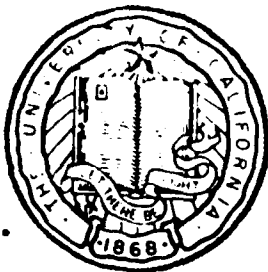
F/G 8/10

NL





MICROCOPY RESOLUTION TEST CHART
NATIONAL BUREAU OF STANDARDS-1963-A



(12)

PROGRAM IN MARINE PHYSICS
APPLIED TO NAVY UNDERSEA MISSIONS

FINAL REPORT

OFFICE OF NAVAL RESEARCH
Contract: N00014-80-C-0077

Total Award: \$996,292
1 November 1979 through 30 September 1982

Principal Investigators
V. C. Anderson and F. N. Spiess

June 8, 1983

DTIC
SELECTED
SEP 3 0 1983
S E

MPL-U-42/83

This document has been approved
for public release and sale; its
distribution is unlimited.

83 09 29 017

DTIC FILE COPY

MARINE PHYSICAL LABORATORY
of the Scripps Institution of Oceanography
San Diego, California 92152

UNCLASSIFIED

SECURITY CLASSIFICATION OF THIS PAGE (When Data Entered)

REPORT DOCUMENTATION PAGE		READ INSTRUCTIONS BEFORE COMPLETING FORM
1. REPORT NUMBER MPL-U-42/83	2. GOVT ACCESSION NO.	3. RECIPIENT'S CATALOG NUMBER
4. TITLE (and Subtitle) PROGRAM IN MARINE PHYSICS APPLIED TO NAVY UNDERSEA MISSIONS		5. TYPE OF REPORT & PERIOD COVERED Final Report
7. AUTHOR(s)		6. PERFORMING ORG. REPORT NUMBER MPL-U-42/83
8. CONTRACT OR GRANT NUMBER(s)		N00014-80-C-0077
9. PERFORMING ORGANIZATION NAME AND ADDRESS University of California, San Diego, Marine Physical Laboratory of the Scripps Institution of Oceanography, San Diego, California 92152		10. PROGRAM ELEMENT, PROJECT, TASK AREA & WORK UNIT NUMBERS
11. CONTROLLING OFFICE NAME AND ADDRESS Office of Naval Research, Department of the Navy, Code 220, 800 North Quincy Street, Arlington, Virginia 22217		12. REPORT DATE 8 June 1983
		13. NUMBER OF PAGES 16 pages
14. MONITORING AGENCY NAME & ADDRESS (if different from Controlling Office)		15. SECURITY CLASS. (of this report) Unclassified
		15a. DECLASSIFICATION/DOWNGRADING SCHEDULE
16. DISTRIBUTION STATEMENT (of this Report)		
<div style="border: 1px solid black; padding: 5px;">This document has been approved for public release under the authority of its distribution to the public.</div>		
17. DISTRIBUTION STATEMENT (of the abstract entered in Block 20, if different from Report)		
18. SUPPLEMENTARY NOTES		
19. KEY WORDS (Continue on reverse side if necessary and identify by block number) underwater acoustics, residual noise field, sound propagation, signal processing, internal wavefield, hydrodynamic noise field.		
20. ABSTRACT (Continue on reverse side if necessary and identify by block number) This final report is a summary of the core program at the Marine Physical Laboratory. The overall core program addresses in a coordinated way the acoustic, hydrodynamic and magnetic environments of the ocean and the opportunities or constraints which knowledge of the environment produces in relation to undersea detection, localization and communication. Projects within these sections interacted among one another through sharing of ideas and technological background within the scientific and engineering staff.		

and through sharing of facilities both ashore and afloat. The core program improved in a correlated way both the basic understanding of oceanic phenomena and the generation and testing of concepts for carrying out sensing and communication tasks in the sea in the most efficient manner.

Accession For	
NTIS GRA&I	<input checked="" type="checkbox"/>
DTIC TAB	<input type="checkbox"/>
Unannounced	<input type="checkbox"/>
Justification	
<i>From 50 year</i>	
By	
Distribution/	
Availability Codes	
Dist	Avail and/or Special
A	



S-N 0102-LF-014-6601

PROGRAM IN MARINE PHYSICS
APPLIED TO NAVY UNDERSEA MISSIONS

Dynamic Beamformer
W. S. Hodkiss

Office of Naval Research
Contract: N00014-80-C-0077

University of California, San Diego
Marine Physical Laboratory of the
Scripps Institution of Oceanography
San Diego, California 92093

The concept of coherently processing a drifting sonobuoy array stimulated a proposal by the Marine Physical Laboratory (MPL) to fabricate and operate a dynamically programmable beamformer for cooperative use with the Naval Ocean Systems Center (NOSC) in a program to explore the feasibility of such an array. Funded by the Office of Naval Research (ONR), this cooperative program was named STRAP (Sonobuoy Thinned Random Array Program).

At the time MPL became involved in the STRAP program, a general purpose high-speed minicomputer implementation of the beamformer was being considered. The general purpose computer approach was attractive in that an existing commercial hardware system could be employed, with the algorithm being implemented in software. The major drawback was that, because the multiple elements had to be processed sequentially through the CPU, even with hardware arithmetic only 15 or so beams could be formed in real time. This would have been a valid approach for a research tool - especially where off-line, nonreal-time analysis would suffice. However, it would not provide any demonstration of a technological base for an operational system that could process up to several hundred sonobuoy channels in real-time with enough beams that a full search coverage could be achieved.

MPL proposed that a special purpose processor be designed which would demonstrate the technological capability of forming the required number of beams in real-time. A description of the hardware which was designed and fabricated is given in [1]. The MPL Dynamic Beamformer permits the incorporation of slow changes in element positions and beam steering directions while the beamformer carries out the real-time formation of 1300 beams from 32 input sensors.

After fabrication of the Dynamic Beamformer hardware was completed, MPL participated in two major STRAP sea tests. Subsequently, MPL joined with NOSC in the analysis of those data sets. Essentially, the analysis showed that coherent processing (beamforming) of the data from individual sonobuoy elements was possible with only a minimal reduction in array signal gain due to inaccuracies in localization of the array elements.

References

[1] W.S. Hodgkiss and V.C. Anderson, "Hardware dynamic beamforming," J. Acoust. Soc. Am. 69(4): 1075-1083 (1981). (Appendix A)

PROGRAM IN MARINE PHYSICS
APPLIED TO NAVY UNDERSEA MISSIONS

FLIP/ORB Services
C. B. Bishop

Office of Naval Research
Contract: N00014-80-C-0077

University of California, San Diego
Marine Physical Laboratory of the
Scripps Institution of Oceanography
San Diego, California 92093

Support was provided in the amount of \$300,000, for Research Platforms FLIP and ORB, which maintained their readiness to conduct research operations at sea during this period, for scientists from the Marine Physical Laboratory, Visibility Laboratory and Marine Life Resources Group of Scripps Institution of Oceanography, and from the Naval Ocean Systems Center and Science Applications, Inc.

PROGRAM IN MARINE PHYSICS
APPLIED TO NAVY UNDERSEA MISSIONS

Data Analysis for RUWS Search

F. N. Spiess
Office of Naval Research
Contract: N00014-80-C-0077

University of California, San Diego
Marine Physical Laboratory of the
Scripps Institution of Oceanography
San Diego, California 92093

A three-day deep-tow survey just west of the island of Hawaii was done gathering side-looking sonar data, topographic profiles and photos in an effort to pinpoint the location of the lost experimental work vehicle, RUWS.

Upon return to port the data were processed in several days in order to provide a base for decisions relating to possible future search operations. After reworking the navigation (refinement of transponder net geometry, editing of bad points, etc), the position information was merged with the sounder and pressure gauge data and profiles along the major tracks were generated. The side-looking sonar data were then translated from the raw analog displays to the geographic plot (correction for slant range and track curvature), with notation as to which overlay belongs with each track. Finally, representative photographs were selected and printed to give a qualitative feel for the fine scale nature of the terrain.

These data were then transmitted to NOSC personnel. The end results provided a base (and confirmation of data validity) for subsequent search operations.

PROGRAM IN MARINE PHYSICS
APPLIED TO NAVY UNDERSEA MISSIONS

Supplemental Ship Funding for Ambient
Noise Measurements with ADA
V. C. Anderson

Office of Naval Research
Contract: N00014-80-C-0077

University of California, San Diego
Marine Physical Laboratory of the
Scripps Institution of Oceanography
San Diego, California 92093

A sea trip with ORB and ADA was carried out in December 1980 for the purpose of collecting data on wind generated surface noise. Observations during this trip were made with ADA close to the surface (50 to 70 meters) and with the array focused to near field. Data from the trip has shown isolated events occurring at the surface with deviations from 50 ms to 500 ms over wind speeds of 3-6 knots. A paper is in preparation at the present time.

Hardware dynamic beamforming

W. S. Hodgkiss and V. C. Anderson

University of California, San Diego, Marine Physical Laboratory of the Scripps Institution of Oceanography, San Diego, California 92152

(Received 19 August 1980; accepted for publication 29 December 1980)

The hardware architecture of a programmable, time domain, digital beamformer built by the Marine Physical Laboratory is discussed. The Dynamic Beamformer permits the incorporation of slow changes in element positions and/or beam steering directions while carrying out the real-time formation of 1300 beams from 32 input sensors. The sensors are distributed in an arbitrary but known manner over a maximum aperture of 2 s in time delay, or 800λ at the uppermost operating frequency of 400 Hz. Oversampling the sensor signals by a factor of 2.5 above the Nyquist rate is shown to permit the use of a simple, two-point linear interpolation filter to achieve the time-delay quantization intervals required. Element-(as opposed to beam-) level recording of the original sensor data provides a flexible and compact mechanism for postexperiment data analysis.

PACS numbers: 43.60.Gk, 43.60.Qv

INTRODUCTION

The concept of coherently combining the sensor outputs from a random array of freely drifting sonobuoys stimulated work by the Marine Physical Laboratory to fabricate a dynamically programmable beamformer. As conceived, the drifting sonobuoy array, depicted in Fig. 1, would be a sparse array with average element separations much larger than one-half wavelength at the frequencies of interest. The requirements imposed by this drifting, sparse array were the essence of Dynamic Beamformer design. Being a sparse array, the number of resolvable coherent combinations or beams formed from the individual sonobuoy sensor outputs would exceed by two or three orders of magnitude the number of elements themselves. Being a drifting array with time varying element locations, the beamforming time delays would need to be adjusted dynamically in order to accommodate the changing geometry.

This paper will focus on the design considerations and hardware architecture of the MPL Dynamic Beamformer and not dwell on the statistical theory of random arrays. The theory of random arrays, including the expected value and variance of the array spatial transfer function, the expected beam or power pattern, and the estimation of peak side-lobe level, is covered in detail elsewhere.¹⁻³

Design considerations are based on the practical aspects of implementing the beamforming process. Section I develops the mathematics of time domain beamforming from an array whose elements are located arbitrarily in three-dimensional space. In addition, the number of beams which a sparse array must form to adequately probe the volume is discussed in general terms along with a specific example illustrating beam patterns from a 32-element, roughly planar, random array. Another important practical aspect relates to the effects of time-delay quantization and data interpolation for time domain beamforming. Section II outlines the specific hardware architecture of the MPL Dynamic Beamformer. Included is the format of multiplexing the sensor input data and blocking the beam output data. An example of the bearing response to a broadside sinusoidal signal also is provided as an illustration of per-

formance degradation when data interpolation is not used. Section III comments on the data analysis flexibility available with this programmable beamformer. Lastly, Sec. IV provides a conclusion to the paper.

I. RANDOM ARRAY BEAMFORMING

The Dynamic Beamformer uses a time-delay-and-sum approach to coherently combine the element signals for a particular look direction. A large number of such combinations, or beams, must be generated in real time. The number, in fact, is so large that it becomes a significant factor in the beamformer architecture design. The statistical nature of the side lobes associated with a sparse, random array also must be recognized. Additionally, an important factor in the architecture design is the degree of quantization required in the time delays of the beamforming process. These topics will be pursued in this section.

A. Beamforming

The random arrays under consideration are composed of a three-dimensional distribution of equally weighted, omnidirectional sensors. Their spatial locations are specified in the Cartesian coordinate system of Fig. 2. Although the element positions are random variables, the assumption will be made that for any given array at a specified point in time, the E_n are known exactly.

The beamforming task consists of generating the waveform $b_n(t)$ (or its corresponding sampled sequence) for each desired steered beam direction B_n . Each $b_n(t)$

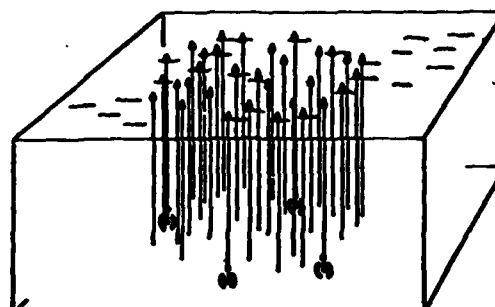


FIG. 1. Random sonobuoy array.

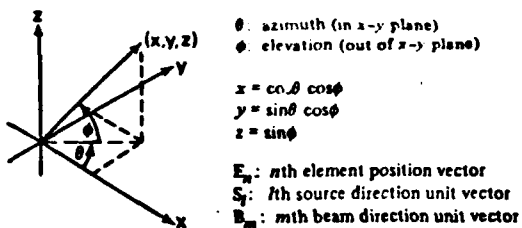


FIG. 2. Coordinate system definition and vector notation.

consists of the sum of suitably time delayed replicas of the individual element signals $e_n(t)$. The time delays compensate for the differential travel time differences between sensors for a signal from the desired beam direction.

Let the output of an element located at the origin of coordinates be $s(t)$. Under the assumption of plane-wave propagation, a source from direction S_i produces the following sensor outputs

$$e_n(t) = s\left[t + (E_n \cdot S_i)/c\right], \quad (1)$$

where c is the speed of propagation ($c \approx 1500$ m/s for acoustic waves in the ocean). Appropriately delaying the individual element signals to point a beam in the direction B_m yields the beamformer output

$$b_m(t) = \sum_{n=1}^N e_n \left(t - \frac{E_n \cdot B_m}{c} \right), \quad (2)$$

$$= \sum_{n=1}^N s \left(t - \frac{E_n \cdot (B_m - S_i)}{c} \right). \quad (3)$$

The vectors involved in the scalar product of one component of (2) are illustrated in Fig. 3. Portrayed is an array of sensors in a plane-wave acoustic field where $B_m = S_i$.

The complexity of the beam formation process arises from the need to carry out the summation in (2) in real time for a large number of B_m directions or beams. In the Dynamic Beamformer, 32 element data inputs are transformed into 1300 beam data outputs. A distinguishing feature of the Dynamic Beamformer is that the

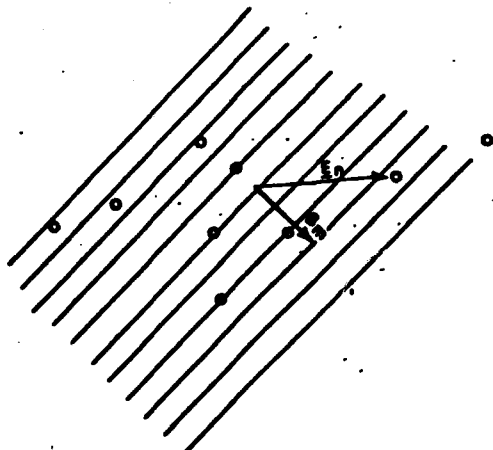


FIG. 3. Element time-delay calculation ($B_m = S_i$).

B_m 's and E_n/c 's are treated as dynamic variables and are allowed to change slowly during the transformation process. As indicated, fluctuations in either or both sound speed c and array element location E_n are mapped into variations within a time-delay coordinate system.

B. Number of beams required

It must be kept in mind that it is the projected aperture of the array in the beam steering direction (B_m) and not the number of elements in the array which determines the beam pattern main-lobe width. Furthermore, the main-lobe width is dependent on the particular planar slice chosen in which the beam vector lies (e.g., horizontal versus vertical beamwidth). In one dimension, the nominal beamwidth is λ/L radians where λ is the wavelength of interest L is the projected aperture dimension.

As an example, consider a planar, circular array lying in the $x-y$ plane of Fig. 2. Given an array whose diameter is D , the nominal horizontal beamwidth would be $\Delta\theta = \lambda/D$ rad. Thus the number of beams which would be required for full edgefire coverage would be $M = 2\pi/\Delta\theta = 2\pi(D/\lambda)$, where (D/λ) is the horizontal aperture dimension in wavelengths.

Consider now a spherical volumetric array whose diameter also is D . In this case, the nominal main-lobe width will be the same in any planar slice chosen in which the beam vector lies. Thus $\Delta\phi = \Delta\theta = \lambda/D$ rad and the corresponding solid angle beamwidth is $\Delta\Omega = \Delta\theta \cdot \Delta\phi = \lambda^2/D^2$ sr. In order to adequately probe all possible horizontal (θ) and vertical (ϕ) angles, the number of beams required would be $M = 4\pi/\Delta\Omega = 4\pi(D/\lambda)^2$.

Figure 4 plots these two values of M as a function of aperture dimension in wavelengths. In actual practice, the random arrays of interest are somewhere between circular planar and spherical volumetric. Further-

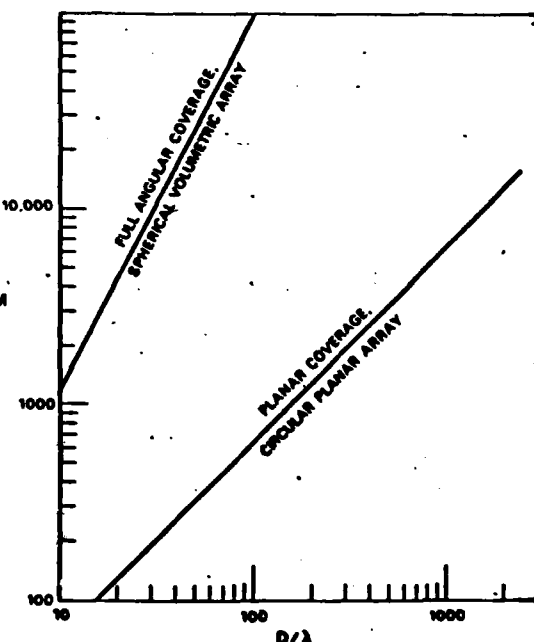


FIG. 4. Required number of beams.

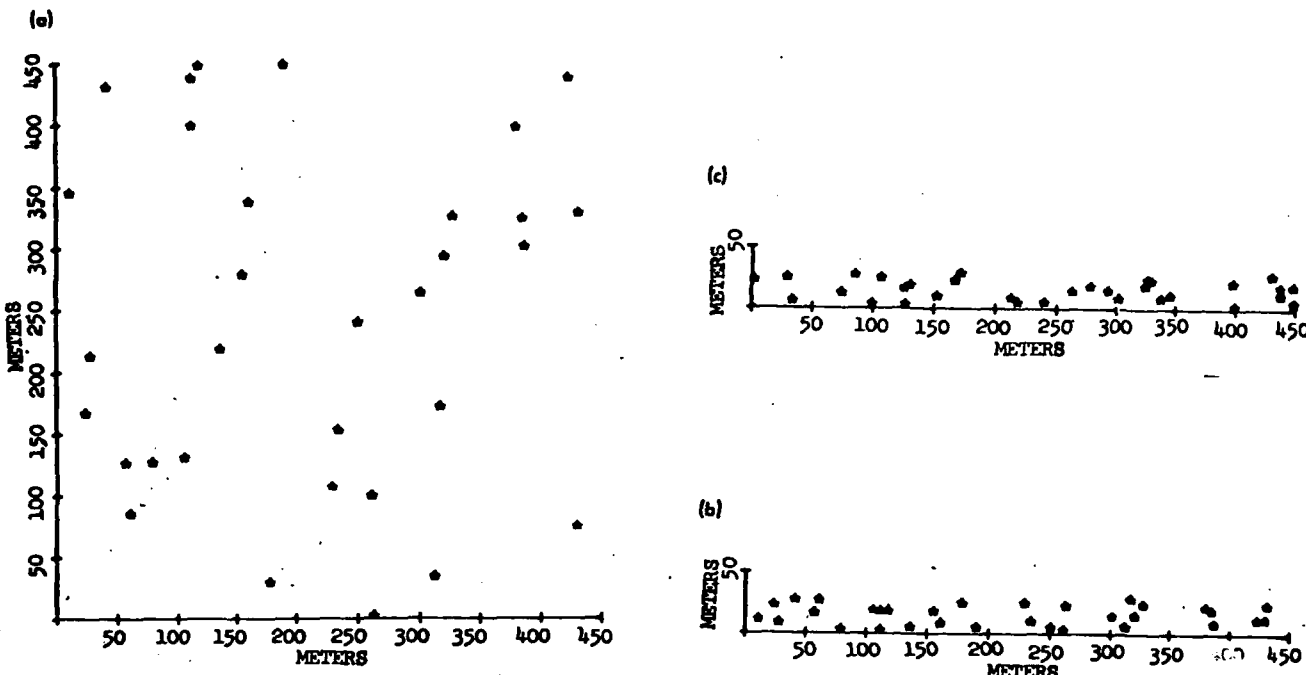


FIG. 5. Random array of 32 elements (a) y versus x , (b) z versus x , (c) z versus y .

more, the patch of solid angle to be investigated typically is neither strictly limited to the horizontal plane nor as large as full angular coverage. Thus the number of beams required in applications of the Dynamic Beamformer would lie somewhere between the bounds indicated in the figure.

C. An example

As a specific example, Fig. 5 shows a single realization of a 32-element, roughly planar, random array. All element locations were assumed independent of one another with identical probability density functions statistically characterizing their individual spatial distributions. Furthermore, the individual distributions were assumed independent and uniform in each dimension of Cartesian coordinates. In this case, array dimensions and frequency are chosen such that $L_x = L_y = 15\lambda$ and $L_z = 1\lambda$. Beam patterns corresponding to these element locations are illustrated in Fig. 6 for an edge-fire beam pointing in the $\theta = \phi = 0^\circ$ direction. The three-dimensional plot has a floor set at $-10 \log N = -15$ dB which is the expected side-lobe level (with respect to a 0 dB on-axis response) for a random array of $N = 32$ elements. Underscoring the statistical nature of the side-lobe structure, note that several side lobes reach levels greater than this mean value.

D. Time-delay quantization

Time domain digital beamforming begins with sampling of the individual sensor signals $e_n(t)$ in (1). With reasonably sharp low-pass filtering of the analog data, sampling need be carried out only slightly above the Nyquist rate (e.g., 2.5 times the maximum frequency of interest) to avoid aliasing or folding out-of-band spectral components down into the baseband of interest. The scalar product in (2) defines the amount each

sensor signal ideally should be time-delayed to form a beam in the B_m direction. The time delays actually available are determined by the data sampling interval. As will be shown below, it is quantization of the time delays which has a far more serious impact on the sensor signal sampling interval than does the Nyquist rate.

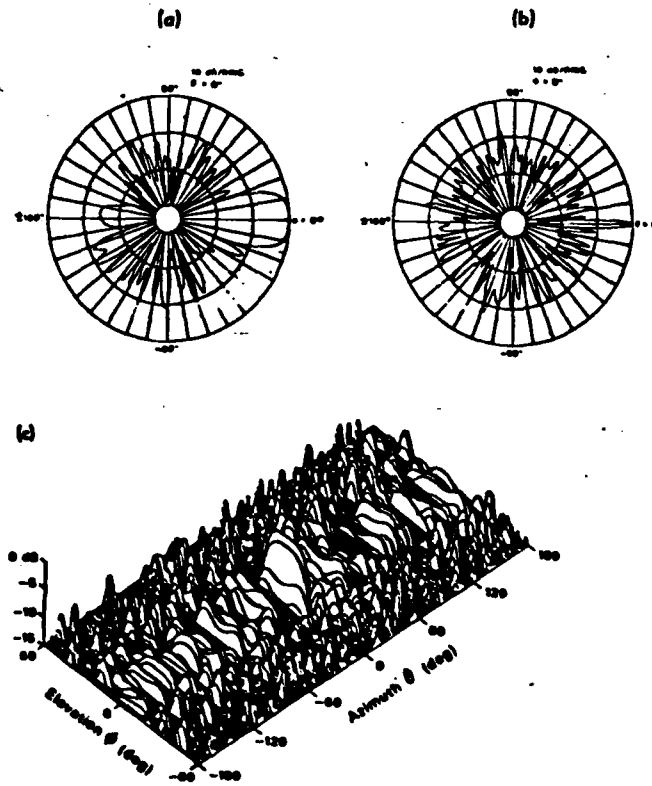


FIG. 6. Random array beam patterns (B_m ; $\theta = \phi = 0^\circ$).

With reference to the development in Sec IA, the ideal array spatial transfer function $A_0(u)$ will be defined as the complex transfer characteristic between $s_i(t) = \exp(j\omega t)$ and $b_m(t)$ in the absence of time-delay quantization. Thus

$$A_0(u) = \sum_{n=1}^N \exp\left(-j\omega \frac{\mathbf{E}_n \cdot (\mathbf{B}_m - \mathbf{S}_i)}{c}\right), \quad (4)$$

$$= \sum_{n=1}^N \exp(j\mathbf{E}_n \cdot \mathbf{u}), \quad (5)$$

where

$$\mathbf{u} = (\omega/c)(\mathbf{B}_m - \mathbf{S}_i). \quad (6)$$

At a given frequency ω , time-delay quantization has the effect of introducing phasing errors $\delta\phi_n$ into the summation in (5). Incorporating these errors, the actual array spatial transfer function is expressed as

$$A(u) = \sum_{n=1}^N \exp(j\delta\phi_n) \exp(-j\mathbf{E}_n \cdot \mathbf{u}). \quad (7)$$

Assuming the phasing errors to be small, replace $\exp(j\delta\phi_n)$ in (7) by the first two terms of its series expansion $(1 + j\delta\phi_n - \delta\phi_n^2/2 + \dots)$,

$$A(u) \approx \sum_{n=1}^N (1 + j\delta\phi_n) \exp(-j\mathbf{E}_n \cdot \mathbf{u}), \quad (8)$$

$$= A_0(u) + j \sum_{n=1}^N \delta\phi_n \exp(-j\mathbf{E}_n \cdot \mathbf{u}). \quad (9)$$

Thus the first order effect of time-delay quantization is an error term (transfer characteristic) added to the ideal spatial transfer function $A_0(u)$.

In many applications, the magnitude squared value of the spatial transfer function is of primary interest and

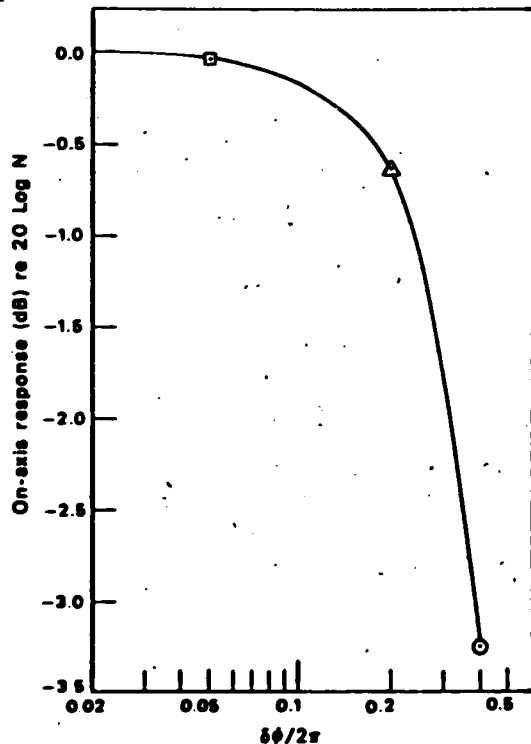


FIG. 7. Time-delay quantization effects.

is generally referred to as the array beam or power pattern. Assuming the $\delta\phi_n$ are zero-mean, identically distributed, and independent of one another, the expected value of the beam pattern is given by^{1,2}

$$E[A(u)A^*(u)] = \alpha A_0(u)A_0^*(u) + N(1 - \alpha), \quad (10)$$

where

$$\alpha = |E[\exp(j\delta\phi_n)]|^2. \quad (11)$$

When the phasing errors are uniformly distributed over the interval $-\delta\phi/2 \leq \delta\phi_n \leq \delta\phi/2$, Eq. (11) evaluates to

$$\alpha = \left(\frac{\sin(\delta\phi/2)}{\delta\phi/2}\right)^2. \quad (12)$$

Furthermore, when $\delta\phi$ is sufficiently small to replace the numerator of (12) by the first two terms in its Taylor series expansion

$$\alpha \approx 1 - (\delta\phi^2/12). \quad (13)$$

Thus the expected value of the beam pattern in (10) can be rewritten as

$$E[A(u)A^*(u)] = \left(1 - \frac{\delta\phi^2}{12}\right) A_0(u)A_0^*(u) + N \frac{\delta\phi^2}{12}. \quad (14)$$

Note that $\delta\phi/2\pi$ corresponds to the fractional data sampling interval with respect to one cycle at the frequency of interest ω .

Errors due to time-delay quantization can be considered separately in two major regions of the expected beam pattern. First, (14) indicates that when N is large the predominant effect in the direction of desired maximum response ($\mathbf{u} = 0$) is an attenuation from $A_0(0)A_0^*(0) = N^2$ by the factor $(1 - \delta\phi^2/12)$. This on-axis loss is illustrated graphically in Fig. 7 as a function of fractional data sampling interval. Indicated with symbols in the expected degradation at the uppermost frequency of interest in the Dynamic Beamformer (400 Hz) for sensor data sampling rates: (1) 1 kHz (circle), (2) 2 kHz (triangle), and (3) 8 kHz (square).

The second region involves the array side-lobe response. The expected beam pattern in this region con-

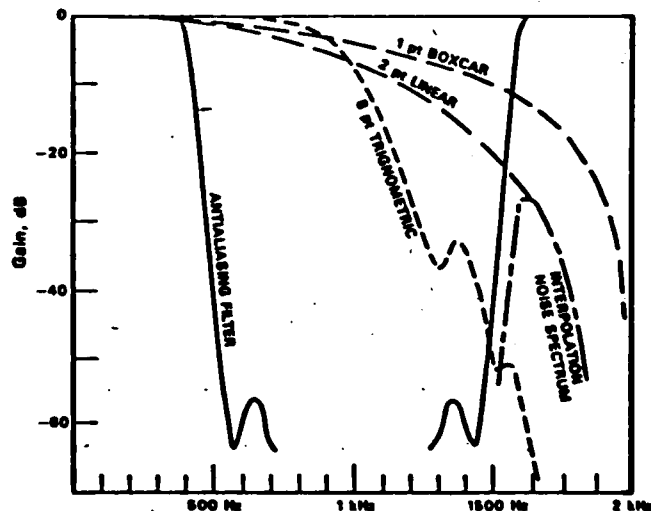


FIG. 8. Antialiasing and interpolation filter response along with the interpolation noise spectrum.

sists of an attenuated version of the side-lobe level in the absence of time-delay quantization effects plus an additive, directionally independent term. Recall that the unnormalized, mean side-lobe level of a random array is N . Thus (14) indicates that time-delay quantization has the average effect of shifting the level of all side lobes towards this mean value.

Since in a random array one has little control over the side-lobe structure due to its statistical nature, the effects of time-delay quantization are of greatest concern in the main-lobe region of the beam pattern. Note from Fig. 7 that in order to preserve an on-axis response to within 0.01 dB of $20 \log N$ for signals at 400 Hz, a sampling rate of 8 kHz is required.

E. Data interpolation

Since the frequencies of interest to the Dynamic Beamformer lie below 400 Hz, antialiasing considerations alone would suggest that a sampling rate of 1 kHz would be adequate. Figure 8 illustrates the frequency response of the 7 pole, elliptic, low-pass filter used to preprocess the individual analog sensor signals prior to digitization. The replicated spectrum centered on the 2-kHz sampling frequency is well separated by this antialiasing filter. In fact, it is evident that even at a 1-kHz sampling rate there would be minimal overlap or aliasing of the spectra. The discussion in Sec. I D has indicated, however, that is quantization of the beamforming time delays which has the greatest impact on the required interval between samples. A sampling rate of 8 kHz would be desirable to maintain on-axis response to within 0.01 dB of $20 \log N$ for signals at 400 Hz.

As discussed by others,⁶⁻⁸ digital interpolation of the sampled sensor signals within the beamformer is one means by which the desired sampling rate can be realized. Essentially, by introducing interpolation hardware into the system, increased complexity of the beamformer hardware is being traded-off against reduced complexity of the sensor signal conditioning hardware, bandwidth requirement of the communication link to the beamformer, and density (or volume) of the storage medium used for data archival.

The process of interpolation involves summing weighted versions of the available data samples both preceding and following the instant in time at which an estimate of the original sensor waveform is desired. The accuracy of the estimate depends on several factors: (1) The sampling rate of the original analog data, (2) the number of samples used to form the estimate, and (3) the values of their corresponding weighting coefficients. Interpolation is quite often viewed as a cascade of two operations. First, zero-valued samples are inserted between the original data samples such that the new sequence occurs at the desired rate. The new sequence then is passed through a low-pass filter to attenuate the periodic replications of the original signal spectrum resulting from the zero-padding operation.⁹ This low-pass filter can be implemented as a transversal filter with tap spacings equal to the new sampling interval and tap weights equal to the interpolation coef-

ficients. In the case of the beamformer interpolator, the data rate is not increased. Instead, a sample with a different, interpolated time delay is computed directly for each channel required as input to the beam summation. Once the beam has been formed as indicated in (2), the beam time series sampling rate will be reduced to a value commensurate with the Nyquist rate for the highest frequency of interest. As a result, the attenuated replications of the original single element spectra fold back into the desired low-frequency region of the beam spectrum and can be viewed as interpolation noise.

Considering a sensor signal sampling rate of 2 kHz (twice the rate which would be adequate for the 400-Hz upper cutoff in the Dynamic Beamformer), Fig. 8 illustrates the attenuation characteristics of three candidate interpolation filters.¹⁰ Although the 2-kHz sampling rate is well in excess of that required to insure minimal aliasing of the individual sensor spectra, that frequency was selected to provide sufficient separation of the sensor spectra replications so that a two-point linear interpolator can be used. Linear interpolation involves the simple combination of a single data sample on either side of the desired sampling instant and requires a negligible increase in the complexity of beamformer hardware. The resulting spectral shape of the attenuated, periodic replication of the individual sensor spectrum is identified in Fig. 8 as the interpolation noise spectrum and is seen to have a peak of 28 dB below that of the desired low-frequency region of the beam spectrum.

II. A HARDWARE DYNAMIC BEAMFORMER

In the selection of a particular hardware architecture for a digital time-domain beamformer, a number of interacting considerations come into play. Included are (1) data sampling rate, (2) interpolator design, (3) size of the time-delay memory field, (4) additional memory for block processing, and (5) number of beams to be formed. The particular choices made for the MPL Dynamic Beamformer will be outlined in what follows.

A. Specifications

Specifications for the MPL Dynamic Beamformer are provided in Table I. The impact of time-delay quantization error considerations and interpolation filter complexity is reflected in the selection of a 2-kHz basic

TABLE I. Dynamic Beamformer specifications.

Bandwidth	10-400 Hz
Number of channels	32
Sampling rate	2 kHz
Interpolation-linear	8 kHz
Maximum time delay	2.048 s
Block buffer	6.144 s
Number of beams	1300
Memory	16 KB \times 32 channel = 500 KB
Data recording	9 Track digital 45 ips 1600 bpi NRZ 10.8 min/2400 ft. Reel

sampling rate which then is interpolated further to an effective 8-kHz rate by the use of a simple linear interpolation operation.

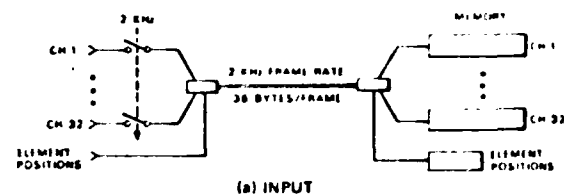
The large number of beams formed in parallel by the Dynamic Beamformer is a consequence of its intended use to process sensor data from a sparsely filled random array. Recall from the discussion in Sec. 1B that it is the aperture of the array and not the number of array elements which determines how many beams are required to adequately probe large sectors of space.

In any experimental program, it is almost mandatory that some means of data recording be provided for later off-line analysis. A first impulse might be to record the output of the signal processor. However, in this case, where 32 sensor signals are transformed into 1300 beams, each with the same data rate, 45 times more recording capability would have to be provided in order to store the output rather than the input data. Thus a recording capability for the digitized individual sensor signals has been incorporated into the total system.

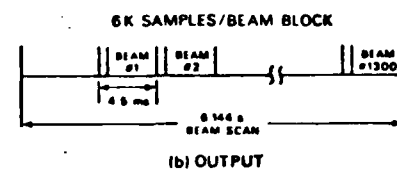
A photograph of the Dynamic Beamformer along with its tape deck and communication terminal is given in Fig. 9.

B. Data relationships (input/output)

The structure of data flow into and out of the Dynamic Beamformer is illustrated in Fig. 10. As shown in Fig. 10(a), after signal conditioning the 32 sensor input channels are sampled in parallel (1 byte/sample). Both the element coordinate data and the 32 channels of acoustic data are formed into a basic 36-byte block consisting of a sync byte (FF), and element identifier byte (the value of "n" in Fig. 2), two bytes of element location vector coordinate data (the value of "x," "y," or "z" in Fig. 2), followed by the 32 bytes of sensor data samples corresponding to one instant in time. The resulting 2-kHz frame rate, 36 bytes/frame, ungapped data stream is both sent to the Dynamic Beamformer memory (where it is demultiplexed) as well as recorded



(a) INPUT



(b) OUTPUT

FIG. 10. Data relationships (input/output).

ded continuously on a 9-track, 45 ips magnetic tape drive at a density of 1600 bpi.

The large memory field provided for each channel in the Dynamic Beamformer enables the formation of beam samples in blocks of 6-K samples/beam ($K = 1024$). As indicated in Fig. 10(b), each block requires 4.5 ms of real time for generation. Although generated at a high data rate in burst sequences, the beam samples correspond to a real-time sampling rate of 1 kHz which is half the original rate for digitization of the sensor signals. The beam blocks are output consecutively with an entire beam scan requiring 6.144 s for completion. A continuous sequence of samples corresponding to the m th beam can be obtained by first demultiplexing each beam scan, then concatenating together the m th beam blocks from consecutive beam scans.

C. Channel memory field

For each beam to be formed, time-delayed samples of the array element waveforms are obtained from a continuously updated memory bank which provides a random access signal field. There are two constraints which determine a lower bound on the size of this field. First, sufficient memory must be provided for each element to cover the maximum acoustic travel time across the physical aperture of the array. The dimension D/λ of the array (see Sec. 1B) is just the number of wavelengths in the memory field needed to satisfy this requirement. Second, some additional buffer or block storage must be provided. The length of this block memory is determined by the computational burden imposed by the scalar product calculation in (2). The longer the block length, the greater the time available for computing a set of time delays for the next beam to be processed.

These two considerations involved in determining the channel memory field length are portrayed graphically in Fig. 11. The time-delay portion satisfies the first constraint. The cross-hatched areas correspond in length to the block storage portion and represent displaced blocks of memory which contain time-delayed replicas of the sampled element acoustic data. Neglecting interpolation, beamforming as in (2) can be viewed as a simple vertical sum across the displaced memory field.

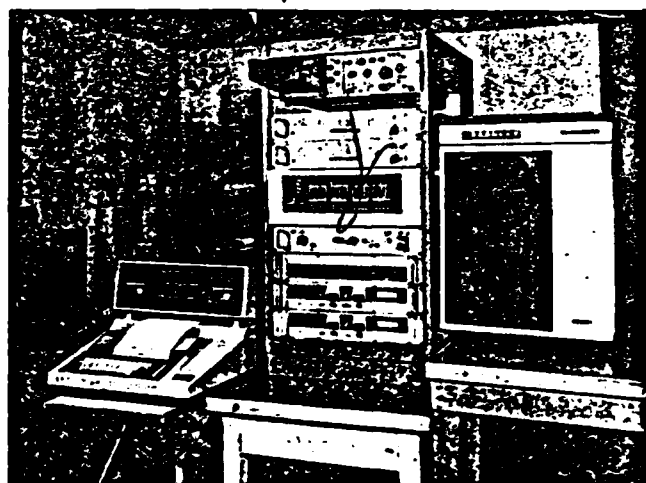


FIG. 9. Photograph of the Dynamic Beamformer tape deck and terminal.

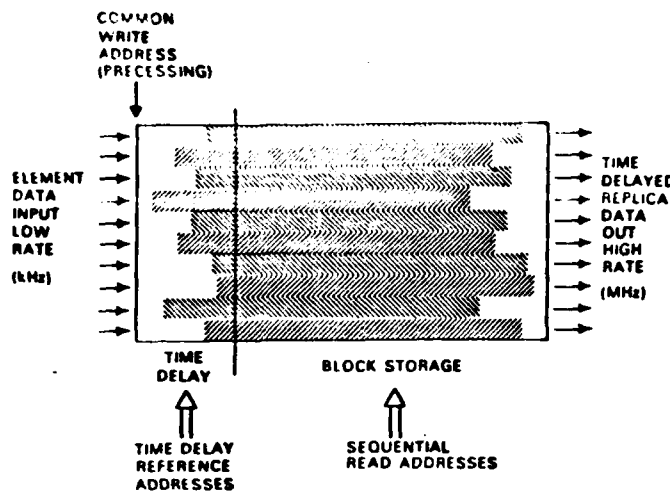


FIG. 11. Channel memory field.

D. Hardware architecture

The basic architecture of the Dynamic Beamformer is shown in Fig. 12. In addition to the 7-pole elliptic low-pass antialiasing filter mentioned previously, the signal conditioning for each channel provides for a common 20-dB gain adjustment and a spectral weighting low-pass filter with selectable cutoff frequencies from 50 to 400 Hz. A bank of sample-and-hold circuits operates synchronously at the 2-kHz sampling rate. The parallel channel amplitude levels are multiplexed, converted to an 8-bit digital sample, then sent on to the data formatter in a serial byte stream. An IEE data bus couples external digital data consisting of array element position and beam vector coordinates into the data formatter. All byte data values are restricted to the range 00-FE (hex) so that FF (hex) can be reserved as a sync byte.

When the tape recorder is running (either in the record or playback mode), the read head output supplies the input to the Dynamic Beamformer. The input is in

the form of an 8-bit acoustic data stream to be demultiplexed in the Element Signal Processing modules (one ESP module for every 8 channels), and a sequence of 16-bit element coordinate values and their identifying addresses to be stored in the program control computer.

Beam output samples are formed by summing appropriately delayed and interpolated channel data samples. Multiple beams can be formed since the beam summation process can be carried out faster than the input acoustic data sampling rate. In the Dynamic Beamformer, the time required for the parallel summation across channels is determined by the memory access rate of 3.2 MHz. Comparing this with the 2-kHz acoustic data sampling rate and allowing some system overhead time, approximately 1500 memory accesses are completed in each 0.5-ms input sampling period. The linear interpolation operation requires two samples from memory. However, since the data rate of the beam output samples only needs to be half the original acoustic data sampling rate, 1500 beam samples are generated for each equivalent output sampling period of 1 ms.

The Dynamic Beamformer can accommodate a differential time delay of 2.048 s which corresponds to 4 KB (KB = 1024 bytes) of memory per channel. An additional 12 KB of memory per channel corresponding to 6.144 s of input data has been provided for block storage. The additional memory makes available time to carry out the scalar products required in (2). These calculations must be repeated each beam scan for every beam since the array element positions and beam vectors are treated as dynamic variables.

Presetable counters are used as address generators for each channel in the memory field. Each one is preset to a starting address which corresponds to the required time delay for that particular array element. The counters then run synchronously at the 3.2-MHz memory access rate for 12-K samples. Allowing some system overhead time, 4.5 ms is required to generate a time compressed burst of the equivalent of 6.144 s

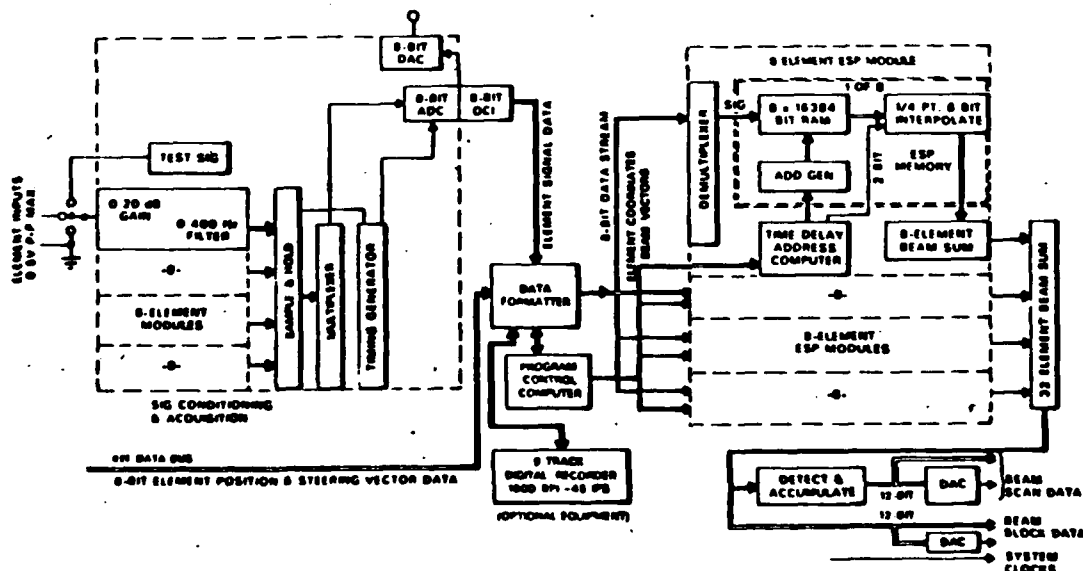


FIG. 12. 32 element Dynamic Beamformer block diagram.

of output data for a single beam sampled at a 1-kHz rate.

During the 4.5 ms interval, four slave microcomputers (one for each ESP module) implement the scalar product in (2) between a new beam vector and a set of element position vectors to generate the time delays for the next beam. Texas Instruments 990/4 16-bit microcomputers were selected for this task. Each 990/4 calculates the time delays for eight elements within the 4.5-ms period. A fifth 990/4 microcomputer augmented by an additional 24 KB of RAM is used as a master controller.

All of the software for the system is resident within the master controller. The element position and beam vector coordinates also are stored there in memory. The scalar product programs are downloaded into the slaves from the master controller over an asynchronous communication link. In the interest of maintaining robust performance in the presence of spurious noise, the slave program memory is reloaded every 6.144 s at the initialization of a new beam scan. This procedure requires 0.294 s and occupies the initial portion of the beam scan graphically portrayed in Fig. 10. In addition, at the beginning of each 4.5-ms beam block, the position vector for one of the eight elements and the vector defining the next beam of the beam scan are downloaded into the slaves.

E. Experimental bearing response

As an aid to check proper operation of the Dynamic Beamformer, provision has been made to input an externally supplied signal to all channels simultaneously. Thus the reception of a broadside arrival by a line array of elements can be simulated.

With a test signal frequency of 200 Hz, detected beam scans resulting when the sensor locations of a 16-element array uniformly distributed along the x axis were loaded into memory are shown in Fig. 13. Array element spacing was 14 ms in terms of time delay which is slightly less than 3λ at this frequency. From left to right in Fig. 13 for this expanded segment of a 1024 beam set, azimuth values (see Fig. 2) start at approximately 83°, pass through 90° (broadside beam) half-way across the figure, and stop at approximately 97°. Each beam is represented by a single point derived by absolute value detecting and accumulating the 6-K beam output samples across an entire beam block (see Fig. 12).

Figure 13 compares the test signal bearing response prior to and after the incorporation of linear interpolation into the hardware. All distortions from a smooth response as a function of azimuth in Fig. 13 are a result of time-delay quantization and are exactly reproducible. Note the significant improvement of the side-lobe response with the addition of $\frac{1}{4}$ -interval linear interpolation.

III. DATA ANALYSIS FLEXIBILITY

A number of features have been incorporated into the Dynamic Beamformer which provide a great deal of flexibility during data analysis. Of primary significance is the capability to interact with the master controller on a real-time basis and thus alter the mode of operation. For example, the master controller issues commands to the magnetic tape recorder calling for forward, fast forward, rewind, or stop. Since this interaction can be with another computer as opposed to an operator, a closed-loop mode of data analysis is possible, where the second computer monitors the output of the Dynamic Beamformer and alters its operation based on what has been learned about the data.

Several specific features which have proven useful include:

- (1) Element masking (selectively turning off any one or group of channels),
- (2) freezing data in memory (successive beam scans work with identical data),
- (3) real-time modification of element locations and beam vectors,
- (4) outputting both the actual beam samples as well as the result of absolute value detecting, then accumulating the entire beam block (the second yields a measure of broadband energy in 6.144 s),
- (5) outputting the individual array element samples as the first 32 "beams" (provides a means by which array signal gain and array gain calculations can be made easily),

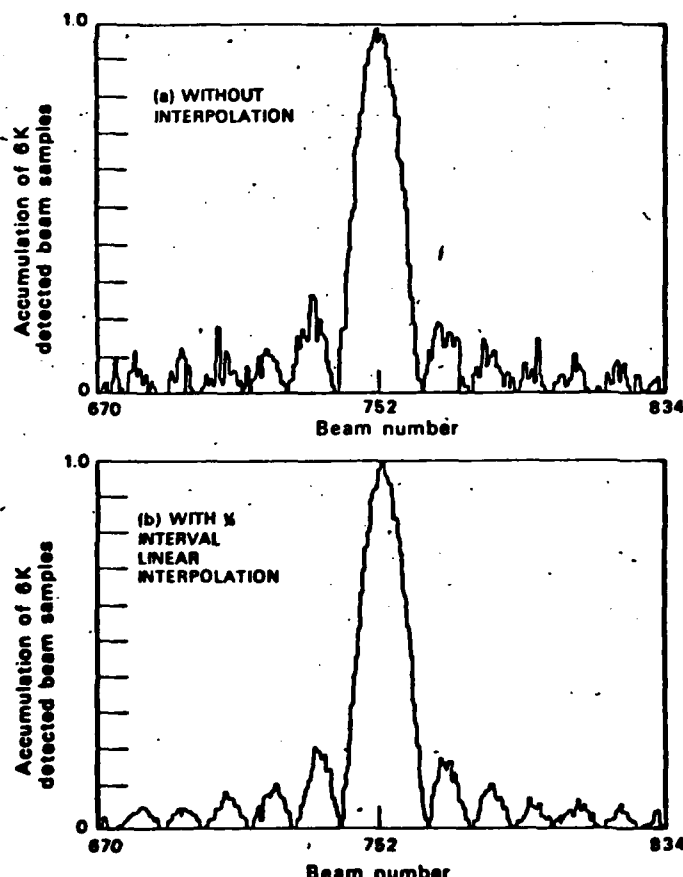


FIG. 13. Dynamic Beamformer bearing response to a 200-Hz broadside test signal.

(6) allowing beam scan reference (starting beam), width (number of beams to output prior to initiating a new beam scan), and dwell (number of consecutive beam blocks to be output which will correspond to the same beam) to be variable.

IV. CONCLUSIONS

The design considerations and hardware architecture of a programmable, time domain, digital beamformer built by MPL has been discussed. The hardware has proven effective in the analysis of data from a sonobuoy thinned random array. Although the hardware which was built is limited to processing 32 sensor channels, the beamformer architecture is amenable to expansion in modules of 8 channels per module.

ACKNOWLEDGMENTS

This work was sponsored by the Office of Naval Research, contract N00014-75-C-0749. The hardware fabrication was carried out by W. R. Cherry of the Marine Physical Laboratory.

- ¹M. I. Skolnik, "Nonuniform Arrays," in *Antenna Theory*, edited by R. E. Collin and F. J. Zucker (McGraw-Hill, New York, 1969) pp. 207-234.
- ²Y. S. Shifrin, *Statistical Antenna Theory* (Golem, Boulder, CO, 1971).
- ³B. D. Steinberg, *Principles of Aperture and Array System Design* (Wiley, New York, 1976).
- ⁴J. V. Thorn, N. O. Booth, and J. G. Lockwood, "Random and partially random acoustic arrays," *J. Acoust. Soc. Am.* **67**, 1277-1286 (1980).
- ⁵W. S. Hodgkiss, "Random Acoustic Arrays," NATO Advanced Study Institute on Underwater Acoustics and Signal Processing, 18-29 August 1980, Copenhagen, Denmark.
- ⁶R. G. Pridham and R. A. Mucci, "A novel approach to digital beamforming," *J. Acoust. Soc. Am.* **63**, 425-433 (1978).
- ⁷R. G. Pridham and R. A. Mucci, "Digital interpolation beamforming for low-pass and bandpass signals," *Proc. IEEE* **67**, 904-919 (June 1979).
- ⁸R. G. Pridham and R. A. Mucci, "Shifted sideband beamformer," *IEEE Trans. Acoust. Speech, Signal Process.* **ASSP-27**, 713-722 (December 1979).
- ⁹A. Peled and B. Liu, *Digital Signal Processing* (Wiley, New York, 1976).
- ¹⁰V. C. Anderson, "Efficient computation of array patterns," *J. Acoust. Soc. Am.* **61**, 744-755 (1977).

DISTRIBUTION

Thomas Warfield
Office of Naval Research
Department of the Navy
Code 220
800 North Quincy Street
Arlington, Virginia 22217 (2)

Director
Office of Naval Research
Branch Office
1030 East Green Street
Pasadena, California 91101

U.S. Naval Research Laboratory
Code 2627
4555 Overlook Avenue, SW
Washington, D.C. 20375 (6)

Director
Defense Documentation Center
(TIMA) Cameron Station
5010 Duke Street
Alexandria, Virginia 22314 (12)

Marine Physical Laboratory
San Diego, California 92152 (2)

END

FILMED

10-83

DTIG